European Review for Medical and Pharmacological Sciences 2015; 19: 4130-4138

Myofibroblastic transformation of rat hepatic stellate cells: the role of Notch signaling and epithelial-mesenchymal transition regulation

Q.-D. ZHANG, M.-Y. XU, X.-B. CAI, Y. QU, Z.-H. LI, L.-G. LU

Department of Gastroenterology and Hepatology, Shanghai General Hospital, Shanghai Jiao Tong University School of Medicine, Shanghai, China

Abstract. – OBJECTIVE: The development of liver fibrosis has been shown to be associated with the transition of quiescent hepatic stellate cells (HSCs) into myofibroblastic HSCs, and the Notch signaling system has been shown to be activated in this process. The Notch signaling pathway is also known to regulate epithelial-mesenchymal transition (EMT).

MATERIALS AND METHODS: In the current study, quiescent HSCs were examined for expression of EMT markers, and experiments were performed to determine whether these markers change as quiescent HSCs transition into myofibroblastic HSCs and whether the process is modulated by Notch signaling. To promote myofibroblastic transition under experimental conditions, enzymatic perfusion and density gradient centrifugation were used to isolate rat HSCs, which were then cultured. A γ-secretase inhibitor was used to inhibit Notch signaling pathway activity in primary rat HSCs.

RESULTS: Upregulated expression of myofibroblastic markers was observed, but expression of quiescent HSC markers and epithelial markers was downregulated during the transition of HSC *in vitro*. Data indicate that expression of the classical EMT marker; i.e., E-cadherin, was decreased and that of N-cadherin and snail 1 increased. Notch 2 and Notch 3 receptors and Hey2 and HeyL target genes expression increased significantly as quiescent HSCs transitioned into myofibroblastic HSCs. When Notch signaling was blocked, however, the myofibroblastic transition of HSCs reverted, and epithelial marker expression was restored.

CONCLUSIONS: Thus, targeting Notch signaling may provide new insights into the mechanism of HSC transition and may offer a possible therapeutic target for the treatment of hepatic injury.

Key Words:
Epithelial-mesenchymal transition, Hepatic stellate cells, Myofibroblastic transformation, Notch signaling.

Abbreviations

α-SMA = alpha smooth muscle actin; BSA = bovine serum albumin; CK-7 = cytokeratin 7; CK-19 = cytokeratin 19; DAPI = 4',6-diamidino-2-phenylindole; DAPT = N-[N-(3,5-difluorophenacetyl)-L-alanyl]-S-phenylglycine t-butyl ester; DMSO = dimethyl sulfoxide; ECL = electrochemiluminescence; EMT = epithelial-mesenchymal transition; GAPDH = glyceraldehyde-3-phosphate dehydrogenase; GFAP = glial fibrillary acidic protein; Hes = hairy and enhancer of split; Hey = hes-related family bHLH transcription factor; HSCs = hepatic stellate cells; MET = mesenchymal-epithelial transformation; MF-HSCs = myofibroblastic HSCs; NICD = Notch intracellular domain; PBS = phosphate buffered saline; PPARγ = peroxisome proliferator-activated receptor-γ; PVDF = polyvinylidene fluoride; Q-HSCs = quiescent HSCs; SD = standard deviation.

Introduction

Virtually all chronic hepatic insults, such as toxicity, viral infection, metabolic disturbances, and immunological factors, cause liver fibrosis[1]. Hepatic stellate cells (HSCs) have been implicated in this fibrogenic process[2-4]. Following liver injury, the HSCs go through transdifferentiation, which is a transition from a quiescent, fat-storing phenotype to a migratory, myofibroblast-like phenotype[4]. This transdifferentiation process occurs gradually and is characterized by the appearance of the skeletal muscle protein alpha smooth muscle actin (α-SMA), loss of vitamin A droplets, and increased cellular proliferation. Synthesis of fibronectin, collagen I, and tissue inhibitor of matrix metalloproteinases also increases4. In contrast, liver fibrosis reverses when myofibroblastic HSCs (MF-HSCs) are induced to either revert to their quiescent state, undergo

Corresponding Author: Lun-Gen Lu, Ph.D; e-mail: lungenlu1965@163.com

apoptosis, or become senescent[3,4]. Understanding the mechanisms underlying phenotypic switching may offer insight useful for the development of antifibrotic therapy.

The Notch signaling pathway is highly conserved among all animal species. Four Notch receptors (Notch 1-4) and five ligands have been discovered in mammals[5]. Signaling upon ligand-receptor binding leads to sequential proteolytic cleavage processes (which can be inhibited by γ-secretase inhibitors) in the Notch receptor extracellular and transmembrane domain to release the Notch intracellular domain (NICD)[5,6]. The NICD subsequently translocates into the nucleus and induces the transcription of its target genes, such as hairy and enhancer of split (Hes) and hes-related family bHLH transcription factor with YRPW motif (Hey)[5]. Increasing evidence suggests the Notch signalling plays a role in the development and maturation of most vertebrate organs[7]. Notch signaling has also been shown to participate in tissue fibrosis in various diseases such as idiopathic pulmonary fibrosis, scleroderma, kidney fibrosis, cardiac fibrosis and liver fibrosis[8]. Moreover, Chen et al[9] reported that blocking Notch signaling was associated with decreased expression of some myofibroblast (MF) genes in an HSC-T6 rat cell line (an immortalized MF-HSC). Epithelial-mesenchymal transition (EMT) is a biological process in which adherent epithelial cells acquire mesenchymal characteristics, promoting migratory and invasive behaviors[10]. EMT is documented to occur in cultured adult hepatocytes, cholangiocytes, and HSCs[11-14]. However, only a few reports[15,16] have described the interaction between Notch and EMT in liver fibrosis.

When freshly isolated HSCs are kept in primary culture using ordinary culture dishes, the cells are activated and undergo a gradual phenotypic transition[17]. During this transition or transdifferentiation, cells increase expression of specific markers, such as α-SMA and collagen I. They also develop novel cellular properties that may be hallmarks for fibrogenic pathogenesis[17,18]. To date, HSC activation has commonly been studied *in vitro* using culture activation as a model for the activation process that HSCs undergo *in vivo*[17-20]. For this reason, the role of Notch signaling in the transition of Q-HSCs into MF-HSCs *in vitro* was examined here, and EMT marker control during this process was assessed for variation as was the potential reversibility of EMT in HSCs.

Materials and Methods

Cell Isolation and Culture

Adult male Sprague-Dawley rats (400-450 g) were obtained for this study (Luwenbio, Shanghai, China). All animals had free access to water and food and were housed in an environment of 30-70% humidity at 18-26°C and a 12 h light/dark cycle. The experiments followed the procedures approved by the Ethics Committee of Shanghai General Hospital, Shanghai Jiaotong University School of Medicine, Shanghai, China.

HSCs were isolated from the liver of male rats by enzymatic perfusion using collagenase IV (Invitrogen, Grand Island, NY, USA) and pronase E (Roche, Shanghai, China) followed by density gradient centrifugation (8.2% Nycodenz, Axis-Shield, Oslo, Norway) of the resulting cell suspension according previously described methods[19]. A medium of 10% serum-supplemented DMEM (Invitrogen) with streptomycin-penicillin (Invitrogen) was used for HSC cultures.

On day 4, primary HSC cultures were treated with γ-secretase inhibitor N-[N-(3, 5-difluorophenacetyl)-L-alanyl-S-phenylglycine t-butyl ester (DAPT, 10 μM; Sigma-Aldrich, St. Louis, MO, USA) for 3 days. Controls were treated with dimethyl sulfoxide (DMSO, Sigma-Aldrich, St. Louis, MO, USA).

Immunofluorescence

Cells were washed twice in PBS and then fixed in 4% paraformaldehyde for 30 min. Next, cells were washed three more times in PBS and permeabilized with 0.5% Triton X-100 (Sigma-Aldrich, St. Louis, MO, USA) for 5 min. Cells were then washed twice with PBS and incubated with 5% bovine serum albumin (BSA) for 30 min. Next, primary antibodies were added and incubated at 4°C for 24 h. Primary antibodies used for HSCs immunostaining were glial fibrillary acidic protein (GFAP, Abcam, Cambridge, MA, USA, diluted 1:200, quiescent HSC marker), and α-SMA (Abcam, diluted 1:100, activated HSC marker). After three washes with PBS, cells were incubated with the following secondary antibodies for 1 h: Alex Fluor 594 donkey anti-mouse IgG or Alexa Fluor 488 goat anti-rabbit IgG (Invitrogen, Grand Island, NY, USA, both at 1:500). Cell nuclear staining was performed with 4', 6-diamidino-2-phenylindole (DAPI) for 5 min and then cells were viewed under confocal laser scanning microscopy (Leica, Mannheim, Germany). Positively stained cells and total nucleat-

ed cells were counted in 10 randomly selected high-power fields. Quantification was carried out in three individual experiments.

RNA Isolation and Real-Time Quantitative PCR (qRT-PCR) Analysis

An RNA Extraction Kit (Takara, Otsu, Shiga, Japan) was used to extract total RNA from newly separated HSCs. Reverse-transcription of total RNA (2 μg) into cDNA was conducted with PrimeScript RT Master Mix (Takara, Otsu, Shiga, Japan). cDNA synthesis was performed at 37°C for 15 min and at 85°C for 5 sec (enzyme denaturation). A SYBR Green PCT Master Mix (Takara, Otsu, Shiga, Japan) kit was used for amplification reactions. Table I lists primer sequences used. An Applied Biosystems ViiA™ 7 real-time PCR system (Invitrogen, Grand Island, NY, USA) was used to perform qRT-PCR. Glyceraldehyde-3-phosphate dehydrogenase (GAPDH) was used to normalize target gene expression.

Western Blot

Proteins were separated by sodium dodecyl sulphate-polyacrylamide gel electrophoresis (SDS-PAGE) and then transferred to a PVDF membrane. Tris-buffered saline containing 0.1% Tween 20 and 3% BSA was used for blocking and then membranes were incubated with primary antibodies followed by incubation with HRP-conjugated secondary antibodies. ECL was used to visualize protein bands (Pierce Biotechnology, Waltham, MA, USA). The primary antibodies α-SMA, GFAP, HeyL, E-cadherin, N-cadherin, cytokeratin 7 (CK-7), and GAPDH were from Abcam, and antibodies cytokeratin 19 (CK-19), Notch 2, and notch3 were obtained from Santa Cruz Biotechnology (Santa Cruz, CA, USA). Anti-Hey2 was purchased from Sigma-Aldrich (St. Louis, MO, USA).

Statistical Analysis

Experimental data are expressed as means ± standard deviation (SD). At least three independent experiments were performed for each experiment. SPSS 21 (SPSS Inc., Chicago, IL, USA) was used for statistical analyses and a Student's *t*-test and one-way ANOVA were used to compare groups ($p < 0.05$ was considered statistically significant).

Results

Primary rat HSC Isolation and Identification

HSCs were isolated from healthy rat livers and, then, cultured for up to 7 days. Freshly isolated

Table I. Primer sets for real-time quantitative PCR.

Gene	Forward primer	Reverse primer	bp	Accession no.
GFAP	CGTCTCAGTTGTGAAGGTCTATT	CAGAAGGATGGTTGTGGACTC	96	NM_017009.2
PPARγ	GAGATCCTCCTGTTGACCCAG	CCACAGAGCTGATTCCGAAGT	129	NM_013124.3
α-SMA	GCTCCAGCTATGTGTGAAGAGG	CAACCATCACTCCCTGGTGTC	151	NM_031004.2
Collagen I	CGGAATGAAGGGACACAGA	ACCTCTCTCACCAGGCAGAC	148	NM_053304.1
CK-7	CCAGCGTGCCAAGTTAGAGT	GCATGAGCATCCTTGATTGC	75	NM_001047870.1
CK-19	GTCTTCCTATGGGGGCATGG	TAAAACTTCCACCGCGTCCT	170	NM_199498.2
Desmoplakin	AGAACACCCTCAGAAAGCGG	TAGGACTACCCTGGTGGAGC	185	XM_225259.8
E-cadherin	CTGGGGTCATCAGTGTGGTC	CTTGACCCTGGTACGTGCTT	183	NM_031334.1
N-cadherin	CTGACTGAGGAGCCGATGAAG	TCTCTCTTCTGCCTTTGTAGACG	101	NM_031333.1
snail1	GGTTCCTGCTTGGCTCTCTT	CAGTGGGTTGGCTTTAGTTCT	157	NM_053805.1
Notch 1	CACCCATGACCACTACCCAGTT	CCTCGGACCAATCAGAGATGTT	186	NM_001105721.1
Notch 2	CTCCAAGCCGTGTATGAACA	TTGATGTCCTCCTCACAGTCC	105	NM_024358.1
Notch 3	TGAGACTGACTTGCTGGACTG	CAATGTGTGCCTGTGTAGCC	114	NM_020087.2
Notch 4	CTCTGTCCGCCTTCTTTCTG	CAAGCACACACCTCCGTTG	156	NM_001002827.1
Hes 1	CGACACCGGACAAACCAAA	GAATGTCTGCCTTCTCCAGCTT	174	NM_024360.3
Hey 1	GCCCTGGCTATGGACTATCG	CGCTGGGATGCGTAGTTGT	146	NM_001191845.1
Hey 2	TGACAGAAGTGGCGAGGTA	CACAGGTGCTGAGATGAGAG	93	NM_130417.1
Hey L	CACAGGTGCTGAGATGAGAG	CACAGGTGCTGAGATGAGAG	119	NM_001107977.1
GAPDH	ATCAACGGGAAACCCATCA	GGTGGTGAAGACGCCAGTAG	108	NM_017008.4

Abbreviations: GFAP: glial fibrillary acidic protein; PPARγ: peroxisome proliferator-activated receptor-γ; α-SMA: alpha smooth muscle actin; CK-7: cytokeratin 7; CK-19: cytokeratin 19; Hes: hairy/enhancer of split; Hey: hes-related family bHLH transcription factor; GAPDH: glyceraldehyde-3-phosphate dehydrogenase.

HSCs were round phase-dense cells containing refractile lipid droplets, as seen under phase microscopy (Figure 1A). The typical rapidly fading blue-green autofluorescence of vitamin A was observed (λ_{328nm}) under a fluorescent microscope (Figure 1B). GFAP-positive cells were 92.3% ± 2.1% of cells viewed and these were quantified by counting cells in 10 randomly selected high-power fields and data from three individual experiments were averaged (Figure 1C). After culture, HSCs lost cytoplasmic retinoid droplets, as determined by phase contrast microscopy (Figure 1E), and autofluorescence (Figure 1F), and they evolved into myofibroblast-like cells, which was confirmed with immunofluorescent staining for α-SMA (Figure 1H).

Changes Epithelial and Mesenchymal Marker Expression After Myofibroblastic Transition of Primary rat HSCs in Culture

RNA and protein were harvested at regular intervals (0, 3, and 7 d). qRT- PCR was used to measure gene expression changes. Myofibroblastic markers, such as α-SMA, and collagen I, were expressed negligibly in freshly plated cells, as expected but their expression subsequently increased. By day 7, expression of these genes were 30-fold greater than at baseline (Figure 2A). Peroxisome proliferator-activated receptor-γ (PPARγ) and GFAP, typical markers of Q-HSCs, were expressed, but they were downregulated over time and virtually disappeared at culture day 7 (Figure 2B). CK-7 and CK-19, which are typical ductal epithelial cell markers, as well as desmoplakin, a ubiquitous component of epithelial junctional complexes, were measured in freshly isolated HSCs (Figure 2C). In addition to their typical quiescence markers, freshly isolated HSCs expressed epithelial cell markers, and expression of these genes decreased as HSCs developed a more mesenchymal phenotype, characterized by robust expression of several myofibroblastic markers (Figure 2C).

Epithelial factor expression was repressed during culture, allowing HSCs to develop a more myofibroblastic and less epithelial phenotype.

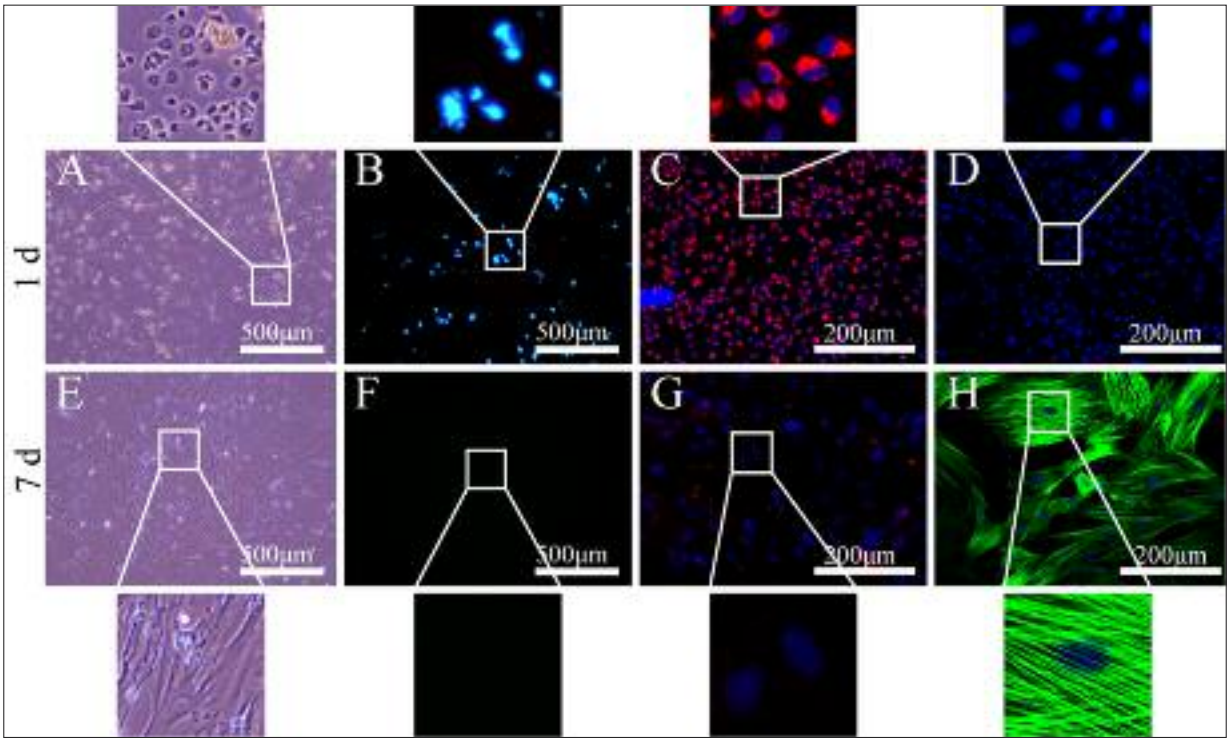

Figure 1. Identification of hepatic stellate cells (HSCs). ***A,*** HSCs appear as round phase-dense cells containing refractile lipid droplets at Day 1. ***B,*** HSCs display typical rapidly fading blue-green autofluorescence at Day 1. ***C,*** HSCs display positive red signals for the quiescent HSCs marker, GFAP, at Day 1. ***D,*** α-SMA expression was almost undetectable in HSCs at Day 1. ***D,*** HSCs lost lipid droplets gradually and transformed into myofibroblasts at Day 7. ***F,*** HSCs lost blue-green autofluorescence at Day 7. ***G,*** GFAP is rarely expressed in HSCs at Day 7. ***H,*** HSCs display positive green signals for the activated HSC marker α-SMA at Day 7. Nuclei stained with DAPI for confocal microscopy.

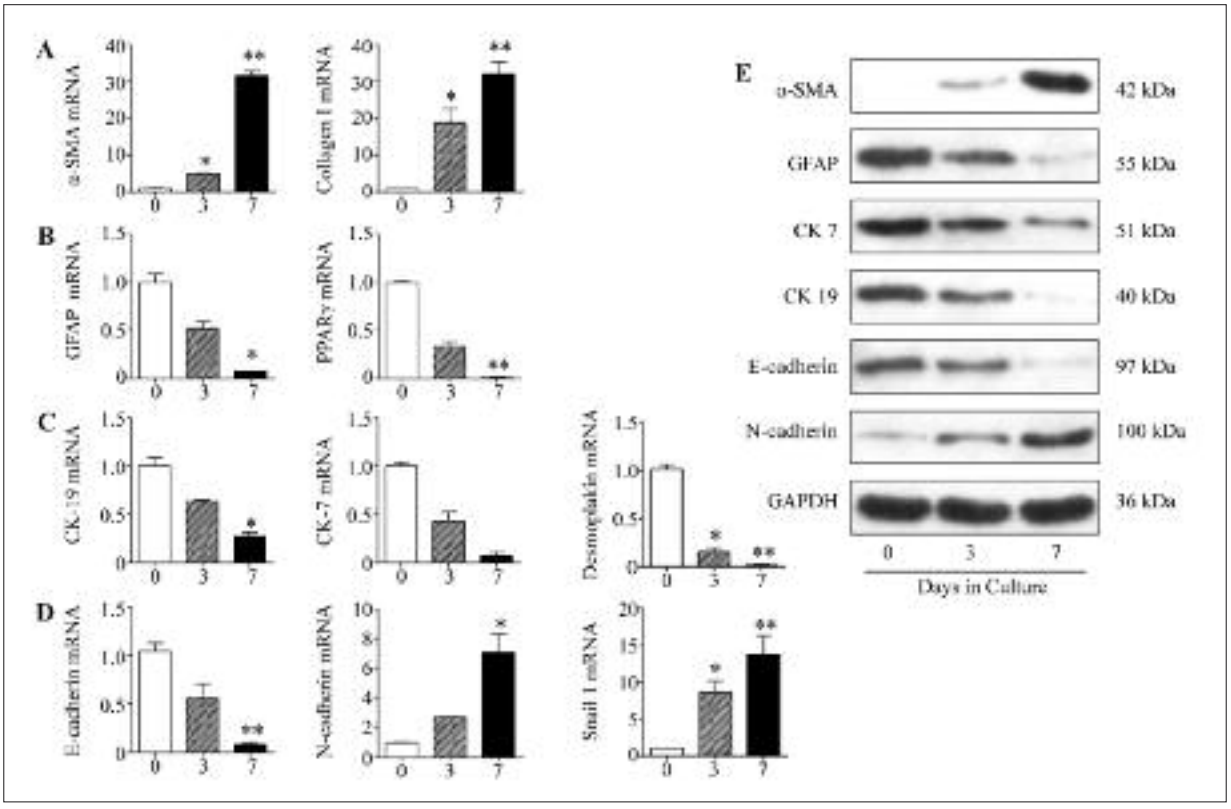

Figure 2. Epithelial and mesenchymal expression changes in culture-induced transition of primary rat Q-HSCs to MF-HSCs. ***A,*** qRT-PCR analysis of myofibroblastic markers: α-SMA, collagen I. ***B,*** qRT-PCR analysis of markers of quiescent HSCs: PPARγ, GFAP. ***C,*** qRT-PCR analysis of epithelial markers: CK-7, CK-19, and desmoplakin. ***D,*** qRT-PCR analysis of epithelial-mesenchymal transition (EMT) markers: E-cadherin, N-cadherin, snail 1. Values are means ± SD of triplicate experiments. $*p < 0.05$, and $**p < 0.01$ vs. 0 Day. ***E,*** Representative Western blot analysis of α-SMA, GFAP, CK-7, CK-19, E-cadherin and N-cadherin from primary rat HSCs. Data are averages of experiments performed in triplicate.

Because phenotypic changes we observed were reminiscent of EMT, we also observed primary HSCs at intervals (0, 3, and 7 d) during cell culture to identify changes in classical EMT markers. Culture-induced transition of HSCs upregulated expression of several factors, including N-cadherin and snail1 and downregulated expression of E-cadherin (Figure 2D). Cell protein changes during culture were tracked with Western blot and data indicated that mRNA expression changes mimicked those alterations at the protein level (Figure 2E). α-SMA and N-cadherin protein in HSCs increased markedly over time in culture, but GFAP, CK-7, CK-19, and E-cadherin expression decreased (Figure 2E). The concept that Q-HSCs have epithelial features was strongly supported by aggregate gene expression changes we observed. Also, data suggest that Q-HSCs underwent an EMT-like process when changing to a myofibroblastic phenotype under standard culture conditions.

Notch Signaling was Up-Regulated During myofibroblastic Transition of Primary Rat HSCs in Culture

We measured Notch-pathway gene expression in freshly isolated primary rat HSCs and in culture-activated MF-HSCs at 3 and 7 days. MF-HSCs had more Notch 2 and 3 expression compared to Q-HSCs (day 0; Figure 3A). Expression of various Notch target genes (e.g., Hes1, Hey1, Hey2, and HeL) were quantified with qRT-PCR to assess pathway changes as Q-HSCs transitioned into MF-HSCs. During HSCs activation, Hey 2 and Hey L mRNA expression increased significantly (Figure 3B). Western blot confirmed that Notch 2 and 3, Hey2 and HeyL mRNA increases were accompanied by increases in related proteins (Figure 3C). Together with other data shown in Figures 2, these findings indicate that the Notch pathway is activated during the transition from an epithelial gene expression pattern to a mesenchymal pattern in primary rat HSCs.

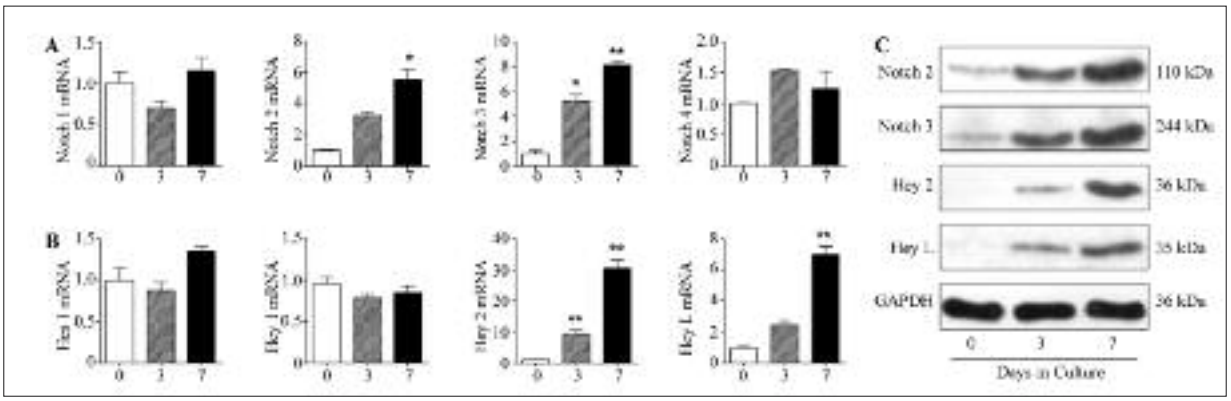

Figure 3. Notch signaling activity occurs with the transdifferentiation of primary HSCs. ***A,*** qRT-PCR analysis of Notch receptors in HSC (Day 0, 3, and 7). ***B,*** qRT-PCR analysis of Notch target genes in HSC (Day 0, 3, and 7). Values are means ± SD of triplicate experiments. *$p < 0.05$, and **$p < 0.01$ vs. 0 Day. ***C,*** Western blot analysis of protein harvested from primary rat HSCs. Results are representative of triplicate experiments. Data are averages of experiments performed in triplicate.

Notch Signaling Differentially Regulated Mesenchymal and Epithelial Markers in Primary Rat HSCs

To investigate the functional significance of Notch signaling in HSCs, primary rat HSCs were cultured for 4 days to induce myofibroblastic transdifferentiation and, then, treated with DAPT for an additional 3 days. As expected, MF-HSC studies confirmed that DAPT treatment significantly reduced mRNA expression of several Notch target genes (Hey 2, and Hey L) (Figure 4A). Western blot confirmed that mRNA suppression was accompanied by decreased protein expression, suggesting that DAPT inhibited Notch signaling activity in culture-activated MF-HSCs.

Blocking Notch signaling in MF-HSCs repressed expression of snail 1 (Figure 4B) and this was accompanied by increased expression of E-cadherin mRNA, and decreased expression of N-cadherin mRNA (Figure 4B) – so-called cadherin switches17. In addition, blocking Notch signaling in MF-HSCs significantly increases epithelial markers such as CK-7, CK-19, and desmoplakin (Figure 4C).

Interestingly, when Notch signaling was inhibited and MF-HSCs reverted to a more epithelial phenotype, expression of myofibroblast genes (α-SMA, collagen I) were downregulated (Figure 4D).

Whole cell proteins were harvested and expression of representative mesenchymal and epithelial markers were quantified with Western blot to verify changes in mRNA expression were accompanied by cellular protein changes. Treatment with DAPT, increased whole cell content of CK-7, CK-19, and desmoplakin protein and inhibited accumulation of α-SMA and collagen I protein (Figure 4E). In addition, Western blot demonstrated that DAPT treatment of MF-HSCs increased expression of E-cadherin protein, and decreased expression of N-cadherin protein (Figure 4E). In summary, blocking Notch signaling in MF-HSCs inhibited the expression of many mesenchymal markers and restored expression of several epithelial markers.

Discussion

Notch 2 and 3 receptor expression was up-regulated as were target genes Hey2 and Hey L when primary rat Q-HSCs transitioned to MF-HSCs *in vitro*. Our findings in primary rat HSCs differ somewhat from those that were reported in an immortalized rat HSC line, which was shown to express mainly Notch 3 and hey 1[9]. This may be the difference between primary and immortal cell lines[17]. However, as were noted in that immortalized rat HSC lines[9], we also found that Notch signal is activated in MF-HSCs. Moreover, we reported that primary MF-HSCs reverted to a less myofibroblastic phenotype when treated with DAPT, a specific Notch-signaling inhibitor. Therefore, Notch pathway activation promotes cell-autonomous transition of Q-HSCs into MF-HSCs, and cells remain myofibroblastic as long as Notch signaling persists. Then, they revert to a more quiescent and epithelial phenotype when Notch signaling is inhibited.

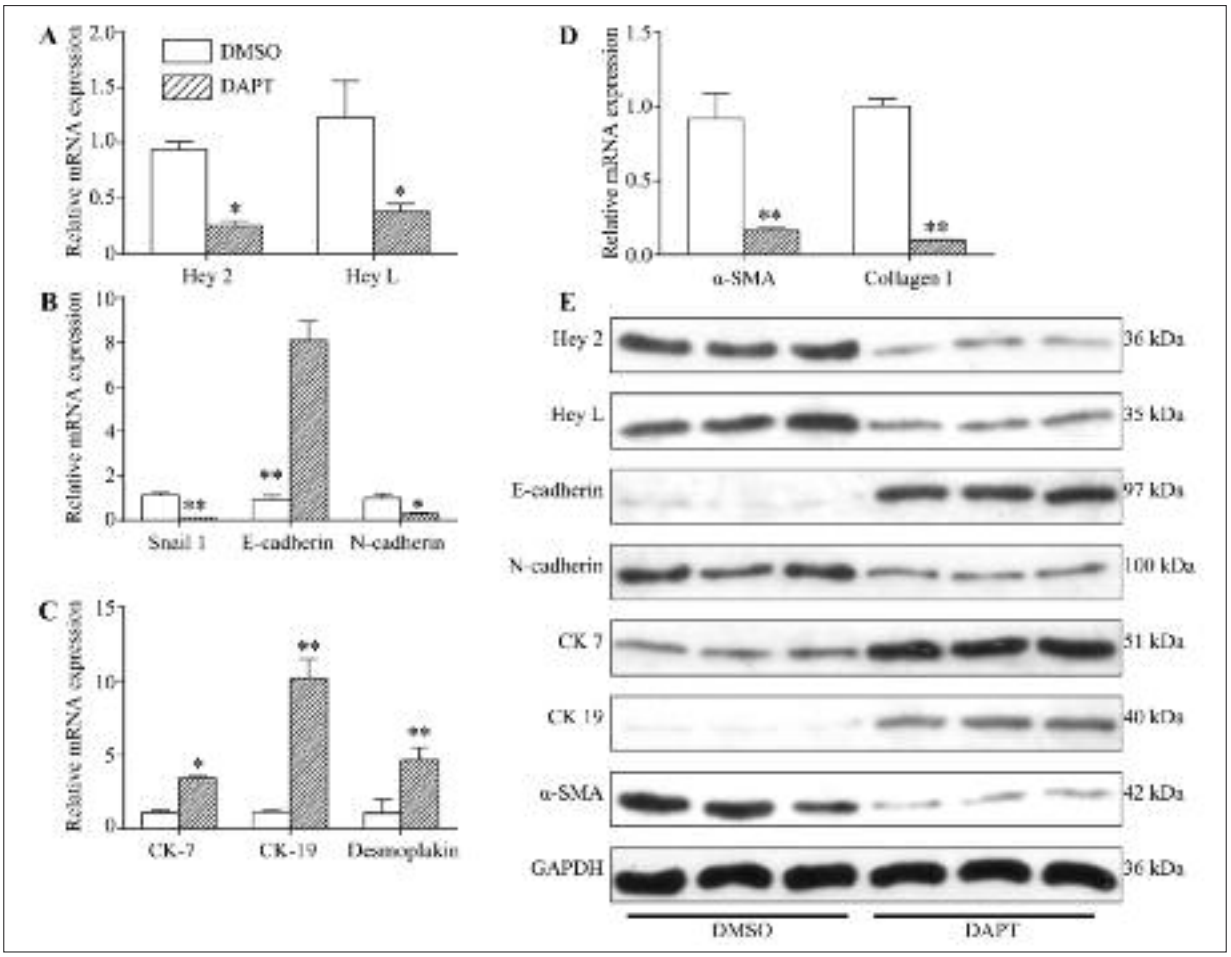

Figure 4. Notch signaling inhibition altered epithelial and mesenchymal markers expression in cultured primary rat HSCs. qRT-PCR analysis of primary HSC at Day 4 treated with DAPT (a pharmacological inhibitor of Notch signaling) or DMSO (control) for 3 days for changes in ***(A)*** Notch target genes, ***(B)*** epithelial-mesenchymal transition (EMT) markers, ***(C)*** epithelial genes, and ***(D)*** myofibroblastic markers. $*p < 0.05$, and $**p < 0.01$ vs. DMSO control; n = 3. ***(E)*** Effects of inhibiting Notch signaling on representative epithelial and mesenchymal marker protein expression in cultured primary rat HSCs treated with DAPT. Changes in protein expression of Hey 2, Hey L, snail 1, E-cadherin, N-cadherin, CK-7, CK-19, and α-SMA were quantified with Western blot. Data are averages of experiments performed in triplicate.

We observed that transformation of rat Q-HSCs into MF-HSCs is similar to EMT. Moreover, MF-HSCs may be able to undergo a mesenchymal-epithelial transformation (MET)-like process that permits them to resume a less myofibroblastic, more epithelial phenotype. However, these reports have received considerable skepticism and Q-HSCs are presently not regarded as epithelial cells[21-23]. HSCs are thought to be derived from cardiac-associated mesenchymal cells during liver development. Likely, cardiac-associated mesenchymal cells migrate to nascent liver bud and mingle with infiltrating endodermal progenitors[22,23]. These cells then ultimately reside beneath the mesothelial lining of the primitive liver[22,23]. Such cells express mesenchymal markers and, thus, are generally considered to be mesenchymal[22]. However, our data and data from the work of others[13,14,24-26] suggest that freshly isolated Q-HSCs contain genes that express epithelium-associated keratins and junctional complex components, such as CK-7, CK-19 and desmoplakin. In addition, HSCs have also been shown to form intercellular junctions with hepatocytes and other HSCs *in vitro*[25]. A key characteristic of epithelial cells is their ability to generate adherent cell layers and form cell-to-cell connections[10]. In this light, HSCs have EMT-like properties[13,21].

A hallmark EMT initiation is a change in E-cadherin expression and this is considered to be

a reliable marker for EMT[27]. E-cahderin down-regulation is essential for epithelial homeostasis, and this can lead to decreased expression of additional epithelial markers, such as tight junction proteins, desmosomal proteins and cell polarity components during EMT[28]. Snail 1 is a zinc-finger binding transcription factor, most widely recognized as a suppressor of E-cadherin expression. Snail 1 binds the E-cadherin promoter, repressing its transcription[29]. The cadherins classical subfamily includes N-cadherin, which has five extracellular cadherin modules. N-cadherin has been shown to enhance tumor cell motility and migration, an effect that opposes E-cadherin activity[30,31]. Moreover, study of rat liver fibrosis reveal that resting HSCs express E-cadherin and β-catenin, and that E-cadherin is changed to N-cadherin when HSCs are activated[14]. We therefore chose N-cadherin, E-cadherin, and snail1 as the classical EMT markers in this study. Our data show that a switch in expression from E-cadherin to N-cadherin occurred and Snail1 expression increased during the transdifferentiation of HSCs. This is consistent with previous reports[14]. We also report that inhibition of Notch signaling in MF-HSCs reversed cadherin switching and repressed Snail 1 expression, another finding that agreed with published data[32] regarding renal fibrosis–that inhibition of Notch limited EMT development in human primary tubular epithelial cells.

Primary Q-HSCs from healthy livers that have been cultured in plastic containers with serum-containing medium can promote Q-HSC transition to MF-HSCs. These primary cultures also have been reported to expand myofibroblastic cell populations, an event similar to processes of hepatic fibrosis *in vivo*[17,18]. However, additional *in vivo* research is needed to confirm the findings.

Conclusions

We found that Notch pathway activation is key for the transition of Q-HSCs into MF-HSCs and our data suggest that inhibition of Notch signaling allows MF-HSCs to enter an MET-like process in which they reacquire a more quiescent phenotype. Thus, targeting Notch signaling may provide new insights into the mechanism of liver injury as well as targets for potential therapeutic interventions.

Acknowledgements

This study was supported by the National Natural Science Foundation of China (No. 81270518, 81470858 & 81570547), and the Wang Baoen Liver Fibrosis Research Fund (No. CFHPC20131025).

Conflict of Interest

The Authors declare that there are no conflicts of interest.

References

1) Bataller R, Brenner DA. Liver fibrosis. J Clin Invest 2005; 115: 209-218.
2) Liu M, Peng P, Wang J, Wang L, Duan F, Jia D, Ruan Y, Gu J. RACK1-mediated translation control promotes liver fibrogenesis. Biochem Biophys Res Commun 2015; 463: 255-261.
3) Lee YA, Wallace MC, Friedman SL. Pathobiology of liver fibrosis: a translational success story. Gut 2015; 64: 830-841.
4) Puche JE, Saiman Y, Friedman SL. Hepatic stellate cells and liver fibrosis. Compr Physiol 2013; 3: 1473-1492.
5) Guruharsha KG, Kankel MW, Artavanis-Tsakonas S. The Notch signalling system: recent insights into the complexity of a conserved pathway. Nat Rev Genet 2012; 13: 654-666.
6) Milano J, McKay J, Dagenais C, Foster-Brown L, Pognan F, Gadient R, Jacobs RT, Zacco A, Greenberg B, Ciaccio PJ. Modulation of notch processing by gamma-secretase inhibitors causes intestinal goblet cell metaplasia and induction of genes known to specify gut secretory lineage differentiation. Toxicol Sci 2004; 82: 341-358.
7) Lai EC. Notch signaling: control of cell communication and cell fate. Development 2004; 131: 965-973.
8) Kavian N, Servettaz A, Weill B, Batteux F. New insights into the mechanism of notch signalling in fibrosis. Open Rheumatol J 2012; 6: 96-102.
9) Chen YX, Weng ZH, Zhang SL. Notch3 regulates the activation of hepatic stellate cells. World J Gastroenterol 2012; 18: 1397-1403.
10) Kalluri R, Weinberg RA. The basics of epithelial-mesenchymal transition. J Clin Invest 2009; 119: 1420-1428.
11) Kaimori A, Potter J, Kaimori JY, Wang C, Mezey E, Koteish A. Transforming growth factor-beta1 induces an epithelial-to-mesenchymal transition state in mouse hepatocytes in vitro. J Biol Chem 2007; 282: 22089-22101.
12) Omenetti A, Porrello A, Jung Y, Yang L, Popov Y, Choi SS, Witek RP, Alpini G, Venter J, Vandongen HM, Syn WK, Baroni GS, Benedetti A, Schuppan D, Diehl AM. Hedgehog signaling regulates epithelial-mesenchymal transition during biliary fibrosis in rodents and humans. J Clin Invest 2008; 118: 3331-3342.

13) Dai W, Zhao J, Tang N, Zeng X, Wu K, Ye C, Shi J, Lu C, Ning B, Zhang J, Lin Y. MicroRNA-155 attenuates activation of hepatic stellate cell by simultaneously preventing EMT process and ERK1 signalling pathway. Liver Int 2015; 35: 1234-1243.

14) Lim YS, Lee HC, Lee HS. Switch of cadherin expression from E- to N-type during the activation of rat hepatic stellate cells. Histochem Cell Biol 2007; 127: 149-160.

15) Morell CM, Strazzabosco M. Notch signaling and new therapeutic options in liver disease. J Hepatol 2014; 60:885-890.

16) Geisler F, Strazzabosco M. Emerging roles of Notch signaling in liver disease. Hepatology 2015; 61: 382-392.

17) Tacke F, Weiskirchen R. Update on hepatic stellate cells: pathogenic role in liver fibrosis and novel isolation technique. Expert Rev Gastroenterol Hepatol 2012; 6: 67-80.

18) Van de Bovenkamp M, Groothuis GM, Meijer DK, Olinga P. Liver fibrosis in vitro: cell culture models and precision-cut liver slices. Toxicol In Vitro 2007; 21: 545-557.

19) Mederacke I, Dapito DH, Affò S, Uchinami H, Schwabe RF. High-yield and high-purity isolation of hepatic stellate cells from normal and fibrotic mouse livers. Nat Protoc 2015; 10: 305-315.

20) Reiter FP, Hohenester S, Nagel JM, Wimmer R, Artmann R, Wottke L, Makeschin MC, Mayr D, Rust C, Trauner M, Denk GU. 1,25-(OH)(2)-vitamin D(3) prevents activation of hepatic stellate cells in vitro and ameliorates inflammatory liver damage but not fibrosis in the Abcb4(-/-) model. Biochem Biophys Res Commun 2015; 459: 227-233.

21) Xie G, Diehl AM. Evidence for and against epithelial-to-mesenchymal transition in the liver. Am. Am J Physiol Gastrointest Liver Physiol 2015; 305: G881-890.

22) Asahina K, Tsai SY, Li P, Ishii M, Maxson RE Jr, Sucov HM, Tsukamoto H. Mesenchymal origin of hepatic stellate cells, submesothelial cells, and perivascular mesenchymal cells during mouse liver development. Hepatology 2009; 49: 998-1011.

23) Loo CK, Wu XJ. Origin of stellate cells from submesothelial cells in a developing human liver. Liver Int 2008; 28: 1437-1445.

24) Higashi N, Kojima N, Miura M, Imai K, Sato M, Senoo H. Cell-cell junctions between mammalian (human and rat) hepatic stellate cells. Cell Tissue Res 2004; 317: 35-43.

25) Fischer R, Reinehr R, Lu TP, Schönicke A, Warskulat U, Dienes HP, Häussinger D. Intercellular communication via gap junctions in activated rat hepatic stellate cells. Gastroenterology 2005; 128: 433-448.

26) Choi SS, Omenetti A, Witek RP, Moylan CA, Syn WK, Jung Y, Yang L, Sudan DL, Sicklick JK, Michelotti GA, Rojkind M, Diehl AM. Hedgehog pathway activation and epithelial-to-mesenchymal transitions during myofibroblastic transformation of rat hepatic cells in culture and cirrhosis. Am J Physiol Gastrointest Liver Physiol 2009; 297: G1093-1106.

27) Zeisberg M, Neilson EG. Biomarkers for epithelial-mesenchymal transitions. J Clin Invest 2009; 119: 1429-1437.

28) Moreno-Bueno G, Peinado H, Molina P, Olmeda D, Cubillo E, Santos V, Palacios J, Portillo F, Cano A. The morphological and molecular features of the epithelial-to-mesenchymal transition. Nat Protoc 2009; 4: 1591-1613.

29) Cano A, Pérez-Moreno MA, Rodrigo I, Locascio A, Blanco MJ, del Barrio MG, Portillo F, Nieto MA. The transcription factor snail controls epithelial-mesenchymal transitions by repressing E-cadherin expression. Nat Cell Biol 2000; 2: 76-83.

30) Conacci-Sorrell M, Zhurinsky J, Ben-Ze'ev A. The cadherin-catenin adhesion system in signaling and cancer. J Clin Invest 2002; 109: 987-91.

31) Cavallaro U, Schaffhauser B, Christofori G. Cadherins and the tumour progression: is it all in a switch? Cancer Lett 2002; 176: 123-128.

32) Saad S, Stanners SR, Yong R, Tang O, Pollock CA. Notch mediated epithelial to mesenchymal transformation is associated with increased expression of the Snail transcription factor. Int J Biochem Cell Biol 2010; 42: 1115-1122.